

# **DETECTION OF A RADIOACTIVE POINT SOURCE ON A LEVEL PLAIN**

Project Report

**Urh Trinko**

mentor doc. dr. Miha Mihovilovič

Ljubljana, August 24, 2023

# Contents

<b>1</b>	<b>Introduction</b>	<b>3</b>
<b>2</b>	<b>Code</b>	<b>3</b>
2.1	Simulating a radioactive source . . . . .	3
2.2	Locating the source . . . . .	4
2.3	Examples . . . . .	4
2.3.1	Zig-zag flyover . . . . .	4
2.3.2	Spiral flyover . . . . .	5
<b>3</b>	<b>Analysis</b>	<b>5</b>
3.1	Quality of the simulation and detection . . . . .	5
3.2	Uncertainty in relation to changeable parameters . . . . .	8
3.2.1	Specific source . . . . .	8
3.2.2	Arbitrary source . . . . .	9
<b>4</b>	<b>Conclusion</b>	<b>11</b>

# 1 Introduction

During this project I was trying to simulate the detection of a radioactive source in python. I have studied this problem in its simplest form, meaning the source was a point and the plain on which it was located was level. The simulation was meant to mimic a detector being flown over the surface on a drone or a helicopter. The main goal was to determine how precisely the source can be located for different heights of the flyover, different quality detectors and the duration of the measurements.

## 2 Code

In order to study the effects of the detection parameters on the location of the source I had to simulate a radioactive source in space. The activity decreases proportional to the reciprocal value of the distance from the source squared. This is the inverse square law,  $A(r) \propto \frac{A_0}{r^2}$ , where  $r$  is the distance from the source and  $A_0$  is the activity of the source. Another way to express this, using two activities at two different distances from the source, would be

$$\frac{A(r_1)}{A(r_2)} = \frac{r_2^2}{r_1^2}. \quad (1)$$

The detector which I simulated is not location sensitive, it is only able to record the number of decays at a certain position.

The first step in the coding process was defining all the changeable parameters. I divided these into two categories. The first one was related to the source (such as the activity, type of radiation) and the second one to the detector (the height of flyover, size of the plain...).

### 2.1 Simulating a radioactive source

This is the part of the code which simulates the flight and measurement of the detector over the plain. The source is located somewhere on the surface. The detector stops at certain points and measures the number of decays. The measurement is simulated using the inverse square law while taking into account the randomness of the radioactive decay. In terms of the code this is done the following way. First the activity at the current position of the detector -  $(x, y, h)$  - is calculated :

$$A(x, y) = \frac{A_0 r_0^2}{(x - u)^2 + (y - v)^2 + h^2}, \quad (2)$$

where  $(u, v, 0)$  is the precise location of the source. The detector moves only in the  $x$  and  $y$  directions at a constant height  $h$ . If we compare equations 1 and 2 we see that they are the same. The value in the denominator of the latter is the distance of the detector from the source, while the numerator value is a product of a different distance from the source  $r_0$  squared and the activity  $A_0$  at this distance. The last two values are constants of the simulations. Their specific values are not important, however they must be present in order to simulate the existence of a source.

The next step in the simulation is to take into account the quality of the detector, which is quantified with  $K$ . The value of the factor is between 0 and 1. A lower number means a better detector, which is able to detect more decays. The actual activity measured by the detector is therefore  $A_{det} = (1 - K)A$ .

Next the number of the decays detected at the position is calculated. This is done by multiplying the activity with the time the detector spent at that position (this is a changeable detector parameter). However radioactive decay is a random occurrence. To simulate this the detected number of decays is a number generated from a Poisson distribution, which has the expected value set as the number of decays previously calculated. To get the final number of decays the ones from the background radiation are added. Background activity is one of the changeable parameters, the number of decays from it is calculated the same as for the sources activity.

The final value displayed by the detector is the dose speed. It is measured in sieverts per second and not becquerels. Sievert is a unit of equivalent dose, which is used to represent the effect radiation has on the human body. The dose can be calculated from the number of detected decays multiplied by  $F$ . This factor contains a lot of information. Radioactive activity only tells us the number of decays per unit of time. In order to get the equivalent dose we must bear in mind many factors, such as the energy emitted by each decay, mass and type of the radiated tissue, type of radiation... All of this is stored in  $F$ . The equivalent dose speed is therefore  $H_d = \frac{FN}{dt}$ , where  $N$  is the number of decays detected and  $dt$  is the time of exposure.

## 2.2 Locating the source

This is the code which could be used to locate the source in a real scenario. The code uses the data of the measured dose speeds and its deviations at different positions of the plain. The equivalent dose follows the inverse square law (1) as the activity. A fit function is defined:

$$H_d = \frac{\alpha}{(x - u)^2 + (y - v)^2 + h^2} + \beta. \quad (3)$$

The information present is a set of coordinates  $x$ ,  $y$  and the corresponding measured dose speed. The fit function must be in line with each of the made measurements. This produces a set of equations, the number of which is equal to the number of measured dose speeds. This is an over defined system of equations which is solved with the Levenberg-Marquardt method for least squares minimization. In python this is achieved with the function `curve_fit` from the `scipy` library. The function produces the values and uncertainties of the unknown parameters  $\alpha$ ,  $\beta$ ,  $u$  and  $v$ . The last two are the location of the source.

## 2.3 Examples

The type of the detector flight over the surface effects the measurements made. I simulated two types, a flyover in a zig-zag pattern and a spiral one.

### 2.3.1 Zig-zag flyover

This is the most basic approach to the flyover. The plain is divided into  $N$ -amount of smaller squares - tiles. The detector starts at the bottom left tile and begins moving

in the  $y$  direction. When it reaches the  $y$  edge of the plain it moves one tile in the  $x$  direction. It then continues moving in the opposite  $y$  direction. This process is repeated until all the tiles are covered. The detector stops at the center of each tile and measures the dose speed for the duration  $dt$ . An example of this method for source location is in figure 1.

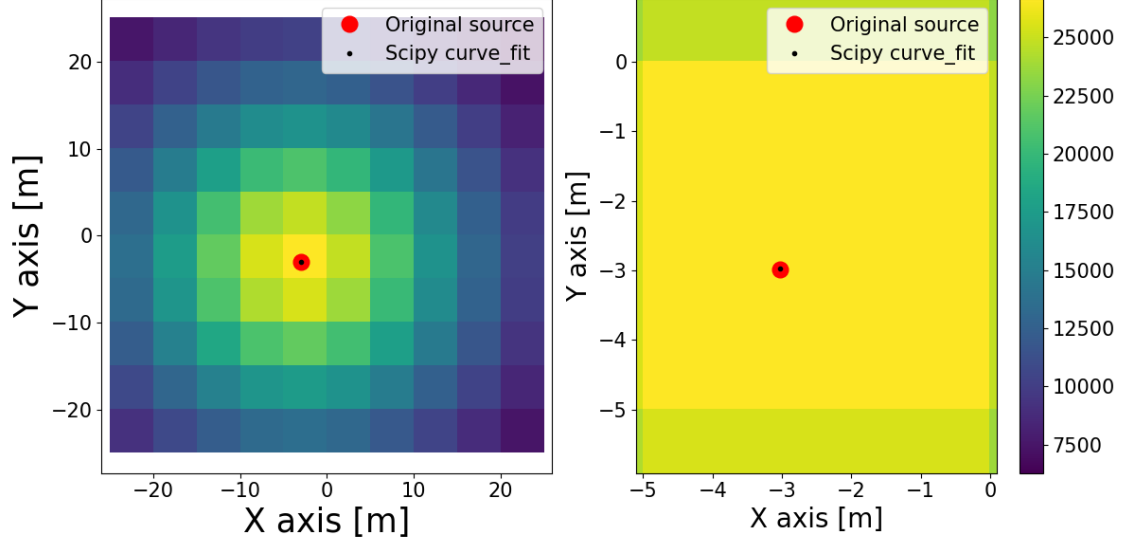


Figure 1: Zig-zag flyover. Tiles colored according to the measured dose speed (left), zoom in on the tile with the highest dose speed (right).

### 2.3.2 Spiral flyover

This flyover method was inspired by the fact that the points with the same activities form circles. So maybe if we measured the dose in a circular motion we would be able to get a more precise result. In this flyover the plain is still divided into tiles. However here the detector first locates the tile with the highest equivalent dose, by moving into the direction of the increasing dose. Once this "hot-spot" tile is located the detector flies outward in a spiral, figure 2.

Whether this method is more precise than the zig-zag is still up for debate. While comparing the precision of each method compared to the amount of measurements made we must take into account the measurements made in the spiral flyover, while locating the "hot-spot" tile. If the source is located closer to the bottom right corner then there will be more measurements made to locate the "hot-spot" tile. However when we do a lot of measurements spiral is usually more efficient, because the amount of measurements in the spiral outweighs the measurements made while searching for the "hot-spot" tile.

## 3 Analysis

### 3.1 Quality of the simulation and detection

I ran two tests to see if the simulation was working properly. With the first one I analysed the deviation of the calculated source location. I ran the code for a source at the center of

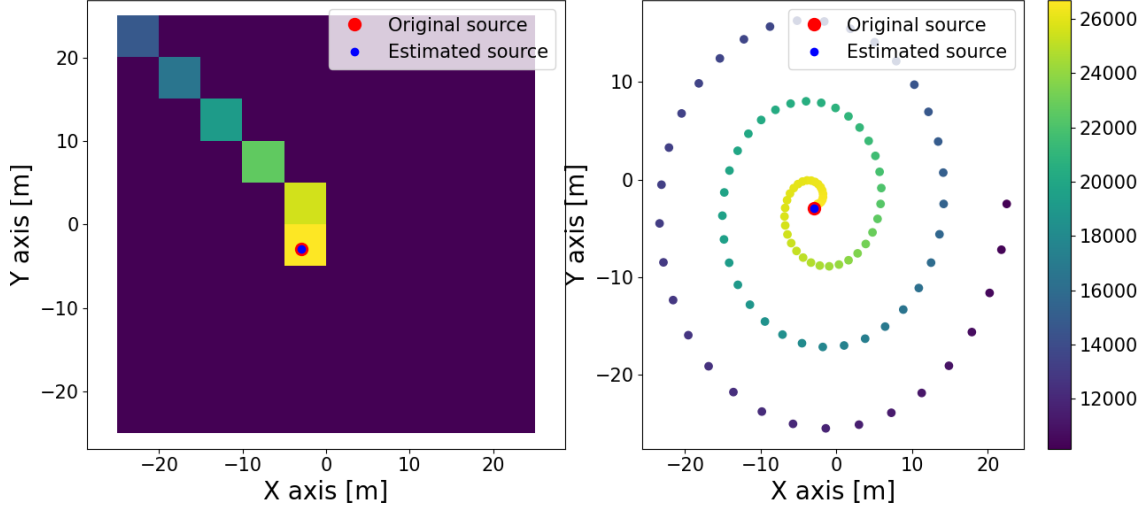


Figure 2: Spiral flyover. Locating the "hot-spot" tile (left) spiral detection making (right).

the plain a thousand times and gathered the data of all the calculated source positions. I sorted this into a histogram, figure 3, and calculated the standard deviation. As it should, the data was distributed around the zero value with a deviation which was similar to the one produced with the curve\_fit function.

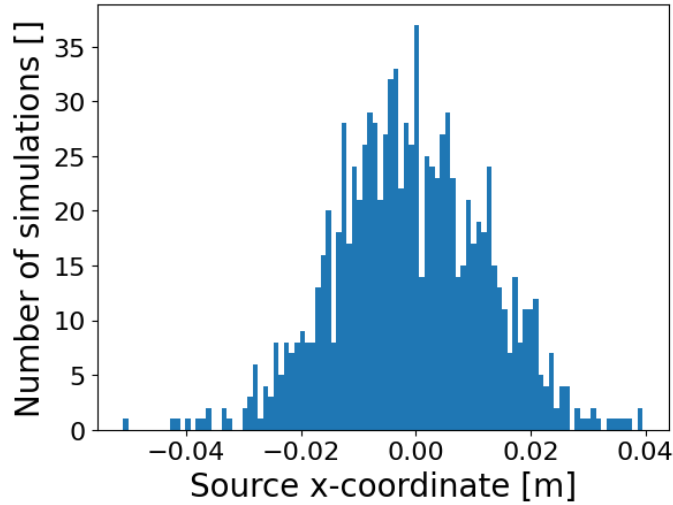


Figure 3: Histogram of the calculated source  $x$ -coordinate for a thousand simulations.

The second test was to simulate the source at different positions of the plain to see if any position has a preference to a higher uncertainty. This would indicate a mistake in the simulation. Figure 4 shows a colored map, where the points represent where the source was generated and the color represents the deviation of the calculated source location.

We can see that the deviation is higher at the edges of the graph. But there is an explanation for this. The flyover method used here was zig-zag. This means that for the sources at the edge the dose was measured at only one side, and so has a larger uncertainty. This idea is further supported by the fact that the  $x$ -deviation and  $y$ -deviation produce different graphs. Less measurements left and right affect the first graph, while less

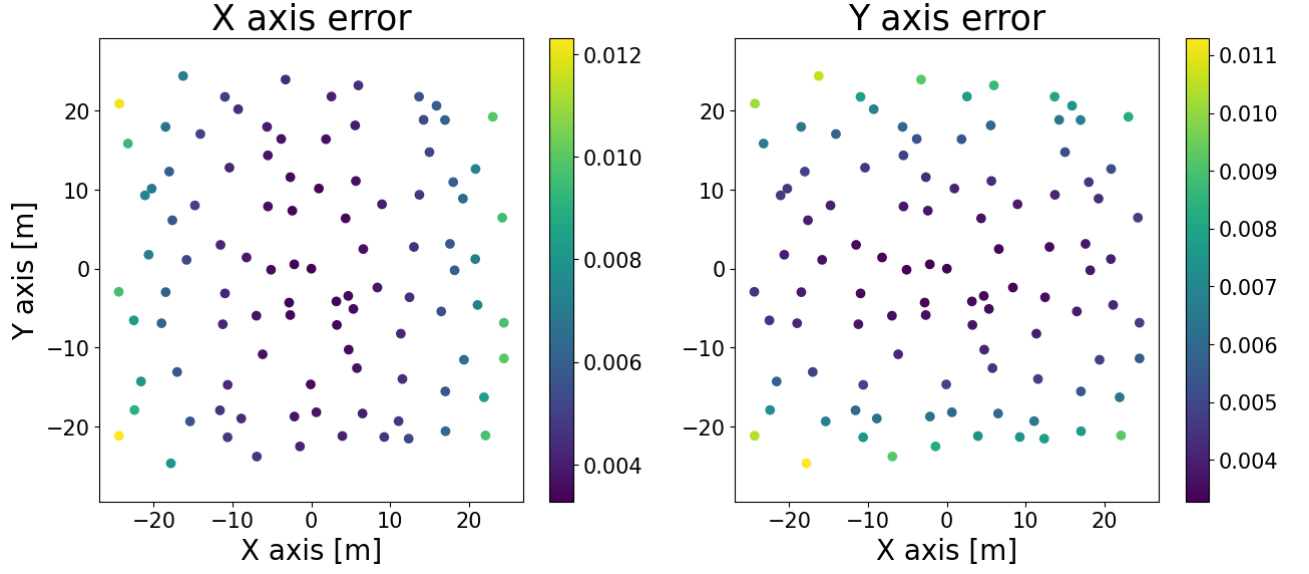


Figure 4: Colored map of uncertainties for  $x$ -coordinates (left) and  $y$ -coordinates (right).

measurements above and below effect the second one. Therefore the first graph has the line of increased deviation on the right and left edge, while the second one has them at the top and bottom of the graph. The points further away from the edges have a mostly uniform uncertainty. Further proof lies in the fact that using the spiral flyover produces a graph which doesn't have this bands of uncertainties at the edges, figure 5, because it always measures around the "hot-spot" tile. This is one of the arguments for this type of flyover over zig-zag.

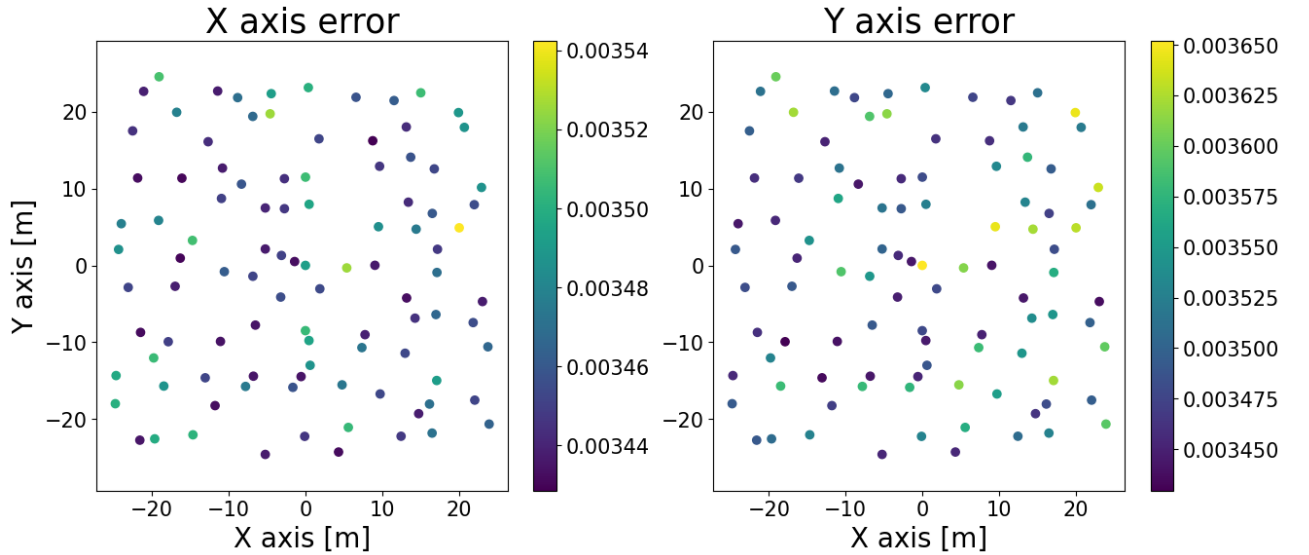


Figure 5: Spiral flyover, otherwise the same as in figure 4.

## 3.2 Uncertainty in relation to changeable parameters

### 3.2.1 Specific source

In this section I will analyse what happens to the precision of source detection if we change the following parameters: detector coefficient, height of flyover and duration of measurement at each tile. Graphs 6a to 6c show how the deviation of the source location changes with this parameters. The graphs show calculations for a source  $u = -14.47$  m,  $v = -8.73$  m,  $r_0 = 50$  m and  $A_0 = 15000$  Bq while the background radiation was  $A_b = 10$  Bq.

From graph 6a we can see that the uncertainty increases as the coefficient  $K$  increases. This makes sense, as a bigger  $K$  means an inferior detector. Such a detector is not able to detect as many of the decays present, which effects the accuracy. Graph 6b displays a similar relation. The uncertainty increases with the height of the measurement. This is also not surprising as the activity from the source we are locating decreases with the height, meanwhile the background radiation is constant. So at greater heights the background negatively effects the location more. Finally, graph 6c shows that a longer duration of measurement at each tile improves the accuracy. This is logical, because a longer measurement means that more information was gathered. Radioactive decay is random and can be described with the Poisson distribution for which the relative error is proportional to  $\frac{\sqrt{N}}{N}$ , where  $N$  is the number of measurements made. As  $N$  increases the relative error decreases because the square rises slower.

By comparing the three graphs in figure 6 we can see that the fastest increase in error happens when the duration of measurement is shorter, which can be equated to a faster speed at which the detector is flying over the surface. This also means that the error decreases very fast when we increase the time of measurement, meaning that it is very important we measure data long enough, or in other words not fly over the surface too fast. We can also make up for a lower quality detector by simply making longer measurements or measuring closer to the ground (more on this later).

We can also see, that the blue dots are higher then the orange ones for the same parameter value meaning that the uncertainty of the source  $x$ -location is larger than for the  $y$ -location. The reason for this is the same as the reason for the sections of higher uncertainty seen in figure 4. Once again the flyover method used was zig-zag. Because the source is located at  $(-14.47, -8.73)$  meters it is closer to the left edge then it is to the bottom, meaning the  $x$ -coordinate will have a higher uncertainty. If we flip the coordinates of the source the graphs will also change so that the  $y$ -coordinate now has a higher uncertainty.

In figure 6 only one parameter is being changed while the other two remain at default values. But the data can be combined to create a three dimensional graph which will display the uncertainty in relation to two adjustable parameters. For example, making measurements on the field when we only have one detector meaning the detector constant cannot be altered. But we can change the height and speed of the flyover. The graph in figure 7 shows how this two parameters effect location accuracy for a source which has the same properties as the one in figure 6. The detectors constant in this example is always equal to 0.1.

From figure 7 we can tell that flying the detector high of the ground and at great speeds produces results with a higher uncertainty. However we can see that even for a 60 meter flyover height the uncertainty is fairly low if the detector is moving relatively slow



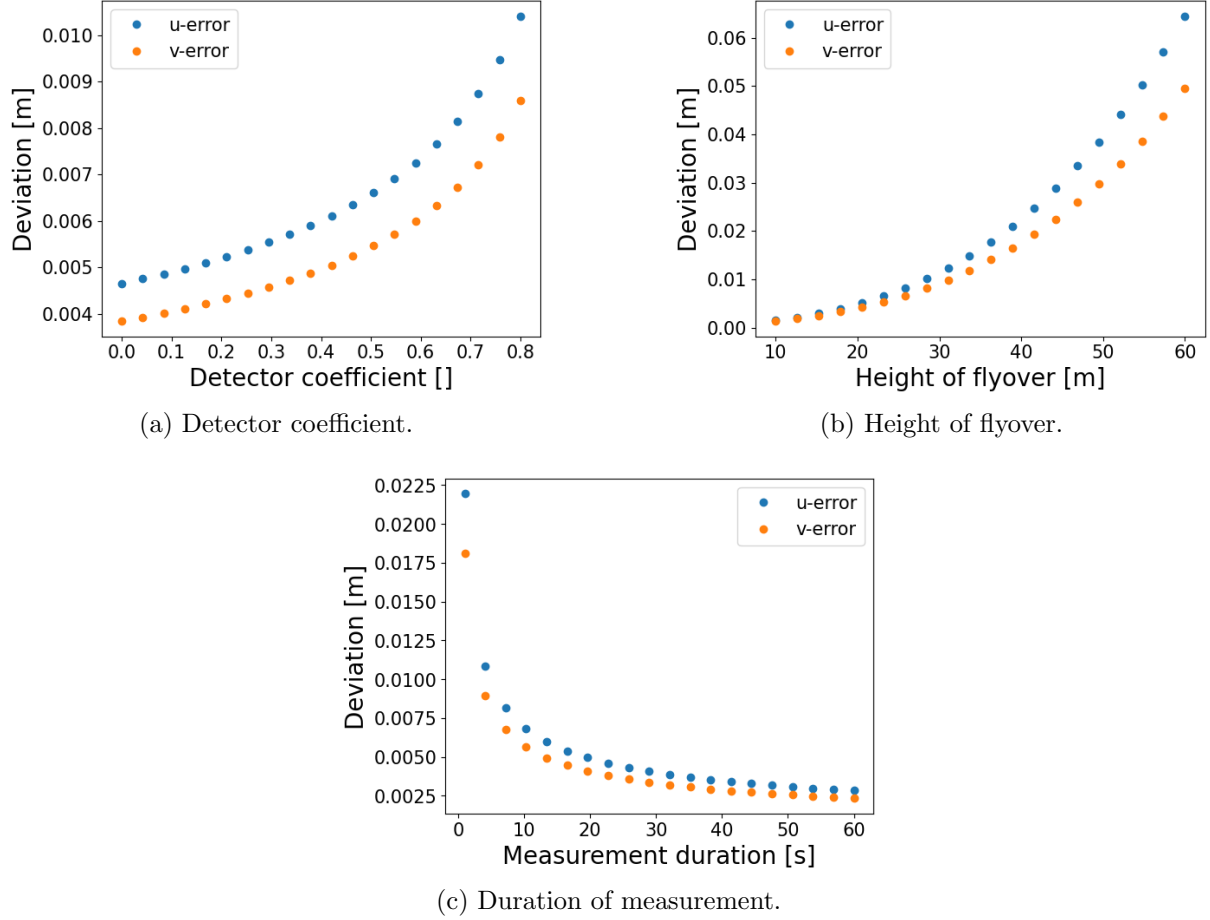


Figure 6: Graphs showing how changing different parameters effects the source location accuracy. The default parameters, values that are constant when one parameter is being changed, are  $K = 0.1$ ,  $h = 20$  m and  $dt = 20$  s.

- equivalent to stopping at the center of each tile for more than 30 seconds. But we must also note that we can decrease the uncertainty of the measurement by increasing the duration only to a certain point. From this point onward the changes in duration won't have a meaningful effect on the uncertainty. While on the other hand the uncertainty can be decreased close to zero by lowering the height of the detector. This is also visible from graphs 6b and 6c. Also the cross section between the plain on the graph in figure 7 and the plain  $h = 20$  m produces, as it should, a line that is similar to 6c.

### 3.2.2 Arbitrary source

Figure 6 represents the relation between the uncertainty and deviation for a specifically located source. In practise it would be more reliable to know this uncertainty for an arbitrary source. This would allow the option to choose the best parameters for measurement and location in advance. With this in mind I ran a similar code that produced the graphs before, but instead of choosing a specific source, I calculated the uncertainty for 25 different source locations spread evenly over the plain. I then calculated the mean and deviation of the gathered uncertainties. The error bars of the graphs in figure 8 therefore

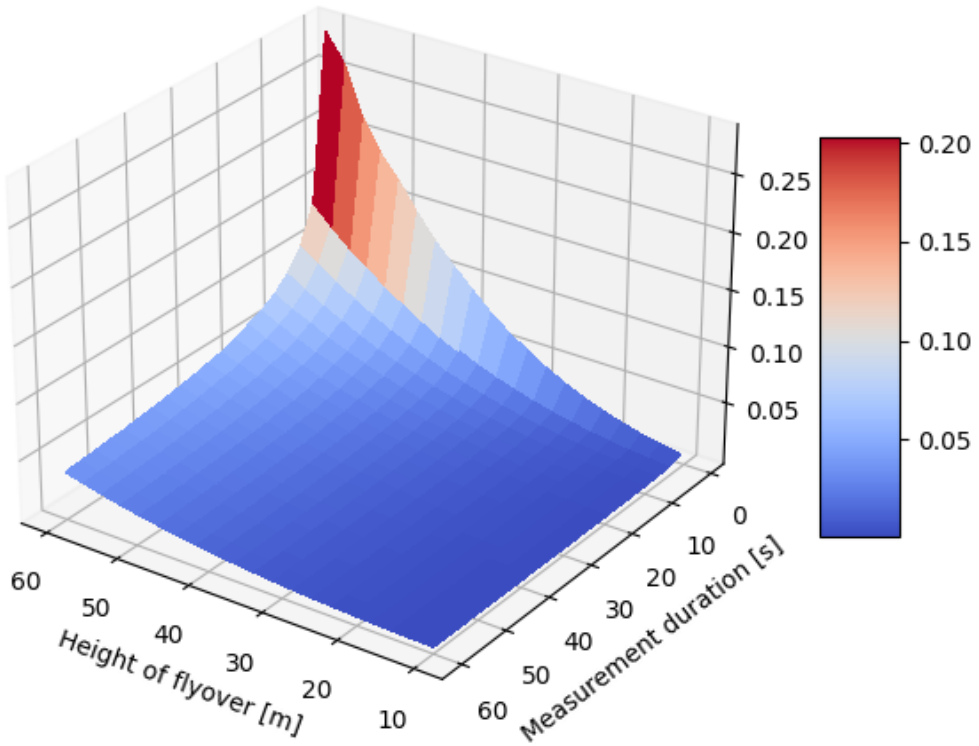
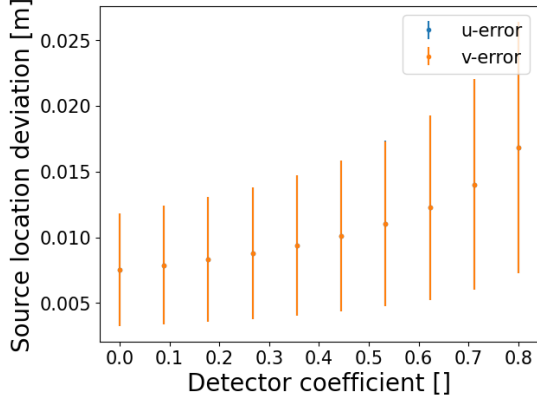


Figure 7: Deviation affected by detector height and speed of flyover. The Z-axis and color map represent the deviation of the calculated  $x$ -coordinate in meters.

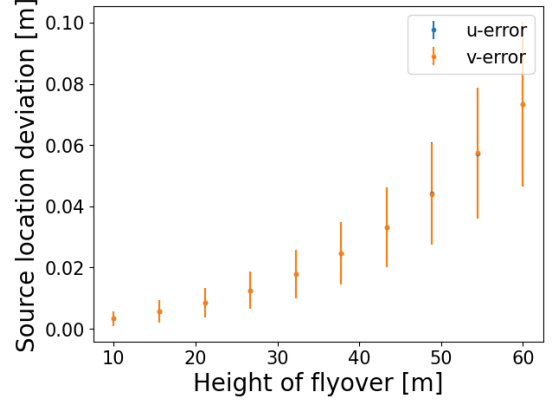
represent a range in which the deviation of the source location would be for general source location. However the other parameters,  $A_0$ ,  $r_0$  and background radiation must be the same as before.

We can see that in this case the dots representing the different coordinates are overlapping, as they should - neither coordinate has a higher/lower uncertainty in general. Also the relation to the changeable parameters is the same as the ones for a specific source in figure 6. In the next step I wanted to do the same as I did in the specific source subsection. Show how the uncertainty changes in relation to the change of the height and speed of the flyover, as in figure 7, but now for an arbitrary source. This time I didn't represent it in the form of a 3-dimensional surface, but as a sort of color-map, with colored boxes that represent the mean location uncertainties and are filled with a number that represents the deviation, previously marked with error bars. In figure 9 there are two such graphs, one for a detector with  $K = 0.1$  and another for  $K = 0.6$ . The only difference is the obvious one, the worse detector produces a higher uncertainty. Note that in this simulation the plain was divided into only 9 equal parts used for calculating the mean and deviation of the uncertainty (opposed to 25 for figure 8). The calculations are otherwise to long.

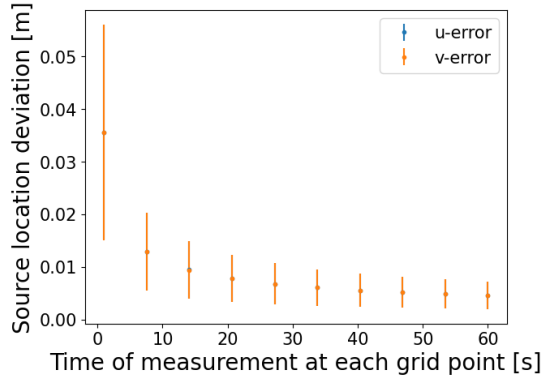
Comparing figures 7 and 9 we can see the similarities. Firstly the uncertainties are the largest for larger heights and shorter duration of measurements. It can also be seen that the deviation from the mean increases with the uncertainty. Secondly the uncertainty drops fast but then stalls for longer measurement duration, as for decreasing the height the uncertainty decreases more constantly. This is in line with the relation to the changeable



(a) Detector coefficient.



(b) Height of flyover.



(c) Duration of measurement.

Figure 8: Same as figures 6a to 6c, but for an arbitrary source location.

parameters shown in figures 6, 8 and 7. Lastly if we compare the graphs for a specific source with the ones for an arbitrary source at the same values  $K$ ,  $h$  and  $dt$ , we can see that the dots in the specific source generally lie inside the interval determined by the arbitrary source code. For example lets look at the values for the parameters,  $K = 0.1$ ,  $h = 20$  m and  $dt = 20$  s. Graph 6c gives us the value 0.005 m while figures 8 and 7 give  $(0.008 \pm 0.004)$  m and  $(0.01 \pm 0.01)$  m respectively. This indicates that the code is working properly.

## 4 Conclusion

In conclusion the emphasis of this report should be on the source location code and the color-map which indicates the interval of uncertainties for an arbitrary source. As mentioned before this kind of map can be generated for any detector coefficient and used to adjust the height and speed of the flyover in order to get the most accurate result with the parameters available.

Having said that there are also some shortcomings which could be improved. For example the `curve_fit` function in the location code is sometimes unable to produce an appropriate fit for the parameters. This becomes especially apparent for higher values of background radiation. This problem often occurs in the code that simulates the location

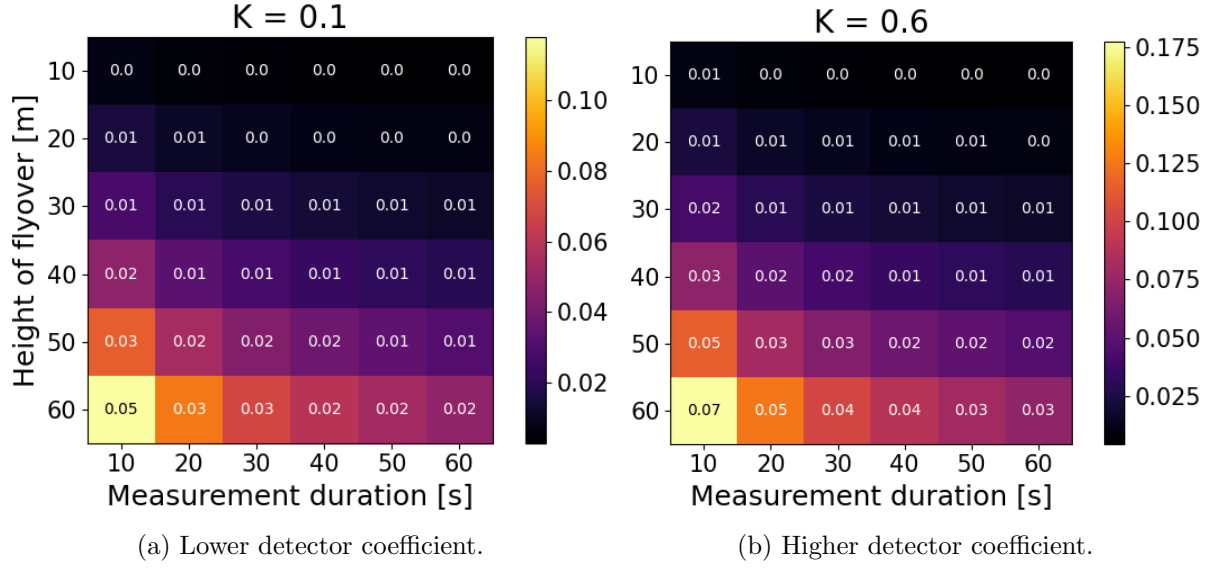


Figure 9: Color-map: color scale represents the mean uncertainty, the writing in each box represents the deviation from the mean.

many times, for example the code that generated the graph in figure 4. Because of this I kept the background radiation relatively low compared to the source activity, while I focused more on the parameters related to the detector. Also related to the color-maps (figure 9) they can only be used for the location of a source whose properties are known, because of the dependence of the code on the constants  $A_0$  and  $r_0$ . Furthermore the issue that is related to both of the ones previously mentioned is the lack of experimental testing of the code. This could however be done. For this I designed GUI-s which can be found in this github repository along with all of the other code used in the making of this project. Lastly a lot of the code relies to much on for loops which makes their run time longer, which is especially apparent when generating the color-map.